Weak magnetic anisotropy in $GdRh_2Si_2$ studied by magnetic resonance

J. Sichelschmidt,[1,*] K. Kliemt,[2] M. Hofmann-Kliemt,[3] and C. Krellner[2]
[1]*Max Planck Institute for Chemical Physics of Solids, 01187 Dresden, Germany*
[2]*Physikalisches Institut, Goethe-Universität Frankfurt am Main, 60438 Frankfurt am Main, Germany*
[3]*Fachbereich Mathematik, Technische Universität Darmstadt, 64289 Darmstadt, Germany*

(Received 10 October 2017; revised manuscript received 25 April 2018; published 20 June 2018)

The antiferromagnetically (AFM) ordered state of $GdRh_2Si_2$ which consists of AFM-stacked ferromagnetic layers is investigated by magnetic resonance spectroscopy. The almost isotropic Gd^{3+} paramagnetic resonance becomes anisotropic in the AFM ordered region below 107 K. The emerging internal anisotropic exchange fields are still small enough to allow an investigation of their magnetization dynamics using a standard microwave-frequency magnetic resonance technique. We could characterize this anisotropy of the excitation at 9 and 34 GHz and found that the material can serve as an interesting illustration of what happens with the dynamics of the order parameter as the anisotropy restrictions become very soft. We have worked out in detail how the magnetic resonance shifts due to a characteristic property of the system, namely, the retardation of the magnetization when the sample is rotated in an external field. To describe the weak in-plane anisotropic behavior, we derived an AFM resonance condition in closed analytical formulas.

DOI: 10.1103/PhysRevB.97.214424

I. INTRODUCTION

$GdRh_2Si_2$ belongs to the silicides with tetragonal $ThCr_2Si_2$ structure which show exceptional magnetic properties, e.g., the antiferromagnetic Kondo systems $YbRh_2Si_2$ [1] and $CeRh_2Si_2$ [2]; $HoRh_2Si_2$, which exhibits so-called component-separated magnetic transitions [3] and a temperature-tunable surface magnetism [4]; and $SmRh_2Si_2$, showing unusual valence states of the Sm ions at the surface and in the bulk [5]. $GdRh_2Si_2$ possesses antiferromagnetic (AFM) order of well-localized magnetic moments appearing below $T_N = 107$ K [6], which is characterized by an AFM propagation vector (001) and a stacking of ferromagnetic layers [6,7]. In spite of the pure spin ground state of Gd^{3+} a weak in-plane anisotropy occurs which is indicated by the magnetization behavior of the ordered moments being aligned in the basal plane. A mean-field model could describe the magnetization data with the assumption that the ordered magnetic moments are aligned parallel to the [110] direction [8].

Recent angle-resolved photoelectron spectroscopy revealed two-dimensional electron states at the Si-terminated surface of $GdRh_2Si_2$ and their interplay with the Gd magnetism. These surface states exhibit itinerant magnetism, and their spin splitting arises from the strong exchange interaction with the ordered Gd $4f$ moments [9].

Magnetic resonance techniques are widely used to study the dynamic properties of magnetic ordering [10]. With $GdRh_2Si_2$ we study a prototypical material which not only exhibits a simple magnetic structure but also allows for the investigation of the magnetically ordered regime with conventional magnetic resonance techniques at low fields and frequencies. We could estimate the temperature dependence of the anisotropy fields from the data by applying a standard condition for the resonance modes in the ferromagnetic sublattices (Sec. III B). However, for the resonance anisotropies observed in $GdRh_2Si_2$ common AFM resonance theories [10,11] turned out not to be applicable because, for instance, the in-plane (a-a plane) anisotropy shows torque effects; that is, the magnetization follows the external field in a retarded way. We refrained from applying the recently reported simulation tool for the complicated case of noncollinear antiferromagnets [12]. Instead, we utilized a mean-field model [8] for the AFM ordering to describe the angular dependence of the resonance field (Sec. III C).

$GdRh_2Si_2$ is best suited to studying the weak a-a plane anisotropy because no hysteresis occurs in the magnetization. This case is rarely reported [13], and to the best of our knowledge, no detailed experimental study of torque effects on the magnetization has been done.

II. EXPERIMENT

High-quality single-crystalline $GdRh_2Si_2$ was used in this study, the growth and characterization of which is described in Ref. [6]. We investigated the paramagnetic resonance (above T_N) and the magnetic resonance of the ordered moments (below T_N) by using a continuous-wave electron spin resonance (ESR) spectrometer together with helium- and nitrogen-flow cryostats allowing for temperatures between 5 and 300 K. Two frequencies, $\omega/2\pi = 9.40$ GHz (X band) and $\omega/2\pi = 34.07$ GHz (Q band), were utilized to evaluate the resonance field condition, which in the paramagnetic region simply reads $\omega/\gamma = H_{\rm res}$, where $\gamma = g\mu_B/\hbar$ is the gyromagnetic ratio and g is the spectroscopic splitting factor.

In general, an ESR spectrometer allows us to measure the absorbed power P of a transversal magnetic microwave field as a function of a static and external magnetic field $\mu_0 H$. A

*joerg.sichelschmidt@cpfs.mpg.de

lock-in technique improves the signal-to-noise ratio by a field modulation which then yields the derivative of the resonance signal dP/dH as the measured quantity. The resulting spectra were fitted with a Lorentzian function including the influence of the counterrotating component of the linearly polarized microwave field [14]. From the fit we obtained the resonance field $H_{\rm res}$ and the linewidth ΔH (half width at half maximum).

III. RESULTS AND DISCUSSION

A. Paramagnetic regime

For the paramagnetic regime, i.e., for $T > T_{\rm N} = 107$ K, the ESR spectra and their temperature dependence was discussed in a recent paper [15]. The spectra display a behavior typically expected for well-defined local moments in a metallic environment with a temperature dependence expected for anisotropic exchange-coupled paramagnets [16–18]. For temperatures near magnetic ordering the critical linewidth divergence could be described by a slowing down of in-plane ferromagnetic fluctuations within a model for a three-dimensional Heisenberg ferromagnet [19].

B. Ordered regime: Temperature dependence

$GdRh_2Si_2$ is a layered antiferromagnet below $T_{\rm N} = 107$ K. The Gd $4f$ moments are ferromagnetically ordered within the basal plane (with alignment parallel to the [110] direction), while they stack in antiferromagnetic order along the [001]-direction [8].

Figure 1 shows selected spectra for the in-plane direction $H\|100$. Upon cooling below $T_{\rm N} = 107$ K the paramagnetic resonance develops into a resonance mode of the AFM ordered system. For temperatures below ≈65 K the spectra consist of more than two lines. The spectral structure indicated by open circles appears near the fields of the spin-flop transition (from magnetization data [6,8], indicated by stars). By sweeping across the spin-flop field the internal field rapidly changes, and during this change it also matches the resonance condition [Eq. (2)], which then leads to the observed structure.

In a narrow temperature region between 55 and 65 K another mode in the $H\|100$ spectra is observed, as indicated by the open squares. We suspect that this mode is part of one of the observed resonance branches.

The spectral structures could be well described by Lorentzian line shapes, which results in the resonance fields and linewidths shown in Fig. 2. For the external field along the easy direction [110], the X-band spectra disappear at temperatures below ≈60 K, whereas the Q-band spectra are well defined down to the lowest temperatures. This means that with decreasing temperature an increasing anisotropy field corresponds to an increasing excitation gap, which below ≈60 K is in between the X- and Q-band frequencies. With increasing the temperature towards $T_{\rm N}$ the anisotropy of the line parameters decreases because the anisotropy field becomes smaller.

The in-plane anisotropy field $H_{\rm A1}$ can be estimated from the resonance field as follows. The conditions [10] of a ferromagnetic (FM) resonance for a sample with cubic crystal structure may be used for an approach to describe the resonance fields for the ferromagnetic planes in $GdRh_2Si_2$. For our case

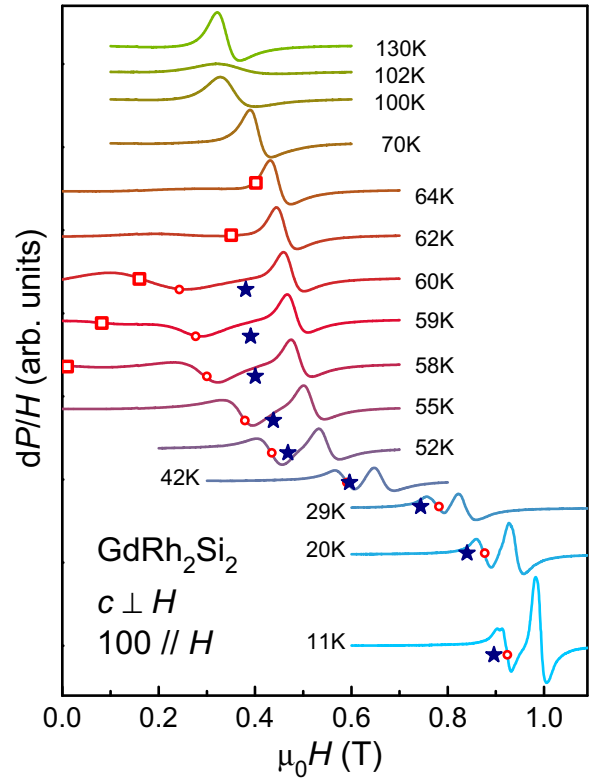

FIG. 1. X-band (9.4 GHz) magnetic resonance spectra at various temperatures, mostly in the magnetically ordered region ($T_{\rm N} = 107$ K), for the external field along the particular in-plane direction [100]. Open squares and circles indicate the resonance fields of additional lines at fields below the main line; see also corresponding symbols in Fig. 2. Stars indicate the spin-flop field as determined from magnetization data [6,8].

with the tetragonal in-plane anisotropy the symmetries are the same as those for the cubic case. With this, we get the resonance conditions which we apply to both FM sublattices in the material: for the easy direction ⟨110⟩,

$$\omega/\gamma = H_{\rm res} + 2H_{\rm A1}; \tag{1}$$

for the hard direction ⟨100⟩,

$$\omega/\gamma = \left[(H_{\rm res} - 2H_{\rm A1})\left(H_{\rm res} + H_{\rm A1} + \frac{1}{2}H_{\rm A2}\right)\right]^{1/2}. \tag{2}$$

Here, $H_{\rm A1,A2} = K_{1,2}/M$ are anisotropy fields, with $K_{1,2}$ being first- and second-order anisotropy constants. From Eqs. (1) and (2) we calculated $H_{\rm A1}$, neglecting $H_{\rm A2}$: for the easy direction ⟨110⟩,

$$H_{\rm A1} = \tfrac{1}{2}(\omega/\gamma - H_{\rm res}); \tag{3}$$

for the hard direction ⟨100⟩,

$$H_{\rm A1} = -H_{\rm res}/4 + \sqrt{\tfrac{9}{16}H_{\rm res}^2 - \tfrac{1}{2}(\omega/\gamma)^2}. \tag{4}$$

Figure 3 shows the results of Eqs. (3) and (4) using the experimental temperature-dependent $H_{\rm res}$. For both in-plane directions the temperature dependencies of the anisotropy fields $H_{\rm A1}$ are similar and thus provide a reasonable estimate of the value for $H_{\rm A1}$. However, they show different

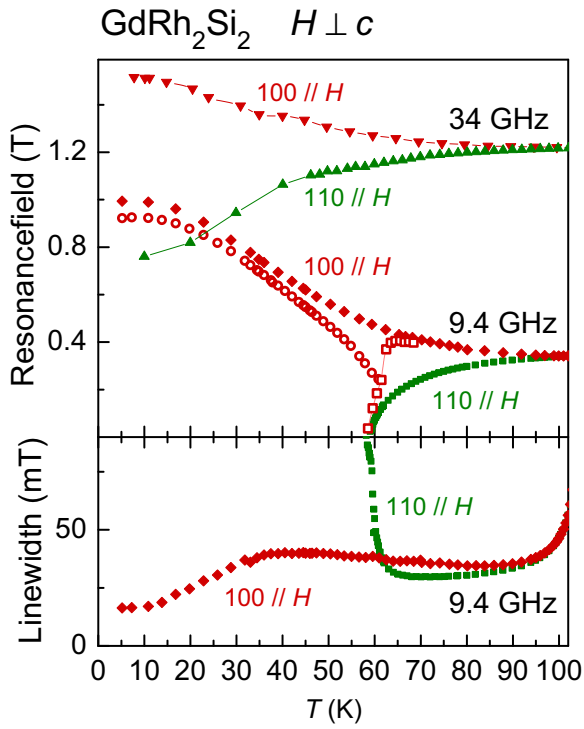

FIG. 2. Temperature dependence of resonance field H_{res} and linewidth ΔH for the external field along two different in-plane directions and two microwave frequencies as indicated. Solid lines guide the eyes. Open squares and circles indicate H_{res} of additional lines, as shown in Fig. 1.

characteristics; the X-band data even seem to cross. This indicates that the basic approach of just using the resonance condition of a FM sublattice as described above is not sufficient to describe our data.

The anisotropy field H_{A1} has to be distinguished from the internal exchange fields which lead to magnetic order. The antiferromagnetic order corresponds to an internal, in-plane exchange field parallel to the [001] direction which is much too large for an AFM resonance mode to be observed at gigahertz frequencies. For $B \| 001$, according to Eq. (A2) in Appendix A,

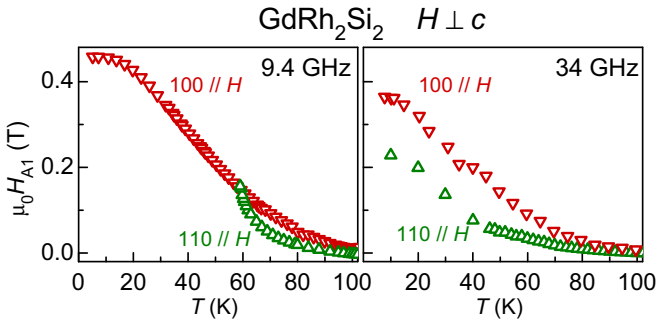

FIG. 3. Calculated temperature dependence of the anisotropy field according Eqs. (3) and (4) for the data at 9.4 and 34 GHz.

the internal field is

$$B^x_{\text{interior,A,B}} = \frac{3k_B}{\mu^2_{\text{eff}}} T_N \sqrt{M^2_{\text{sat}}\left(1 - \frac{T}{T_N}\right) - (\chi_\perp B_z)^2}. \quad (5)$$

Without an external field one obtains for $T \to 0$, $M_{\text{sat}} = 7\mu_B$, $\mu_{\text{eff}} = 8.28\mu_B$, $T_N = 107\,\text{K}$, $B^x_{\text{interior,A,B}} = 48.8\,\text{T}$. Hence, in order to observe an antiferromagnetic resonance a resonance frequency of $\nu = g\mu_B/hB^x_{\text{interior,A,B}} = 1.37\ \text{THz}$ ($g = 2$) is required. This may be hard to verify because terahertz (THz) spectroscopy requires samples with a good transmission for THz radiation, which is not the case for $GdRh_2Si_2$.

The z component of the internal field is solely determined by the external field B_z as

$$B^z_{\text{interior,A,B}} = \frac{3k_B}{\mu^2_{\text{eff}}} \Theta_W \chi_\perp B_z, \quad (6)$$

again using Eq. (A2). One gets with $\chi_\perp(T = 78\,\text{K}) = 0.1\mu_B/\text{T}$ and $\Theta_W = 8\,\text{K}$

$$B^z_{\text{interior,A,B}}/B_z = 0.052. \quad (7)$$

This means that if an external field is applied along the c axis, only ≈5% (at $T = 78\,\text{K}$) is internally available as an effective field for the magnetic resonance. For example, using $B_z = 6\,\text{T}$ from an estimated value $\mu_0 H^{\|}_{\text{res}} = 6\,\text{T}$ of the out-of-plane uniaxial resonance field (Fig. 4, top left frame), one gets $B^z_{\text{interior,A,B}} = 0.31\,\text{T}$. This value is close to the value for the X-band resonance field of Gd^{3+} in the paramagnetic state [15] and also close to the resonance field along the direction [110].

C. Ordered regime: Anisotropy at 78 K

We investigated the anisotropy of the X-band data at $T = 78\,\text{K}$, where the linewidth for the [110] direction shows a minimum (see Fig. 2). The anisotropy of the resonance field and linewidth shown in Fig. 4 is considerably stronger for tilting the external field out of the tetragonal plane (angle Θ, left frame) than rotating it within the plane (angle ϑ, right frame). Interestingly, the out-of-plane anisotropy can be nicely described by a uniaxial behavior (solid lines, left frame), just like a paramagnetic resonance with a uniaxial crystalline field anisotropy (Eq. (1.49a) in Ref. [20]) where the internal field is always aligned along the external field. Also, the above internal exchange-field estimation, Eq. (7), shows that the value of the resonance field corresponds to a typical g value of Gd^{3+}, as observed in the paramagnetic regime [15].

The in-plane anisotropy as shown in the top right frame of Fig. 4 presents a 90° periodicity of both resonance field and linewidth, which reflects the fourfold symmetry in the tetragonal basal plane. The open symbols show the out-of-plane data of the left frame. Obviously, the angular dependencies of both in-plane and out-of-plane data sets are very similar near the easy direction of magnetization, [110]. Such a behavior is not astonishing and can be explained as follows: Magnetization measurements at $T = 78\,\text{K}$ on single crystals yield a spin-flop field $B_{\text{sf}} \approx 250\,\text{mT}$ for a field parallel to the [100] direction and a domain-flip field $B_{\text{df}} \approx 160\,\text{mT}$ for a field parallel to the [110] direction [8]. This implies that for fields of the order of the resonance field, applied along a main symmetry direction, the moments of both magnetic sublattices are in good

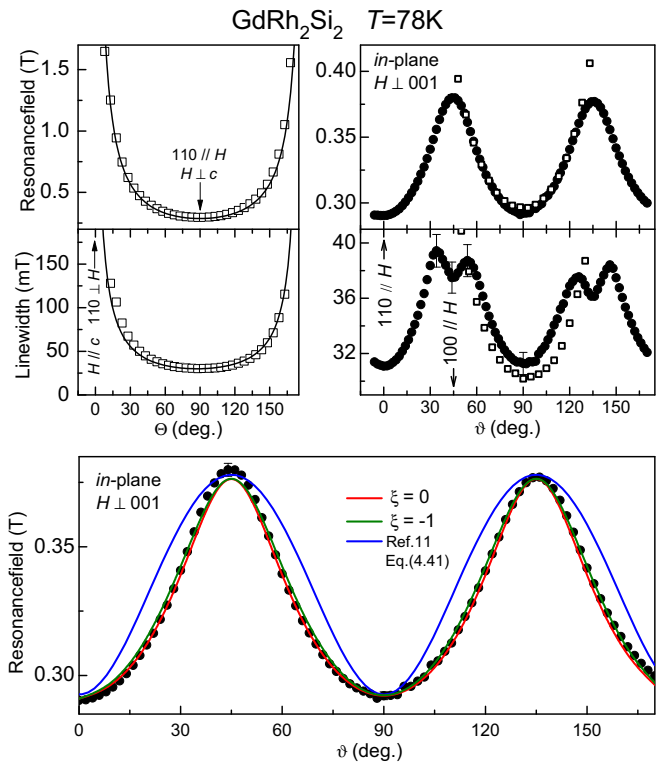

FIG. 4. Angle dependence of X-band resonance field $H_{\rm res}$ and linewidth ΔH; [110] is the easy direction of magnetization. The external field is oriented by angles Θ and ϑ respective of the indicated crystalline directions. Top left: Out-of-plane anisotropy. Solid lines indicate uniaxial behavior with $\mu_0 H_{\rm res}^{\parallel} = 6\,\mathrm{T}$, $\mu_0 H_{\rm res}^{\perp} = 0.29\,\mathrm{T}$ and $\mu_0 \Delta H^{\parallel} = 4\,\mathrm{T}$, $\mu_0 \Delta H^{\perp} = 0.03\,\mathrm{T}$. Top right: In-plane anisotropy with external field H in the basal plane (001) ($c \perp H$) at varying directions. Open squares indicate the data of the left frame. Bottom: Red and green lines indicate $\xi = (\gamma_D/\gamma_M)^2$ with $\xi \to 0$ [best fit according to Appendix B, En. (B9)] and $\xi = -1$ (according to Appendix C). The blue line depicts the expected behavior for a uniaxial antiferromagnet with basal plane anisotropy [11] and instantaneous alignment of the magnetization with the external field.

approximation, aligned perpendicular to that field (Figs. 3 and 5 in Ref. [8]). The magnetic moments can therefore be described as one large domain that extends over the whole single crystal. Upon rotating the field in the basal plane away from a main symmetry direction, the magnetizations of the two sublattices are not equivalent anymore, and a sine-like modulation of the resonance field occurs.

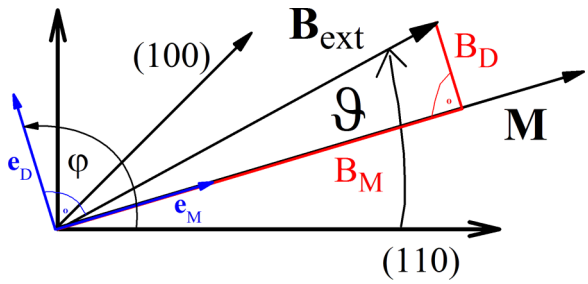

FIG. 5. The choice of the coordinate system.

The in-plane behaviour deviates from a simple sine-shaped curve which is given in the textbook (Ref. [11], Eq. (4.41)) for a tetragonal crystal. The observed deviation is caused by torque effects since the magnetization does not follow the rotating field instantaneously but is retarded. This effect can be studied well in $GdRh_2Si_2$ since no hysteresis in the magnetization interferes with it. In AFM materials hysteresis effects may be due to the switching of magnetic domains or metamagnetic transitions and would result in an asymmetric angular dependence of the resonance field. Such an asymmetry is not observed in $GdRh_2Si_2$.

To model the in-plane behavior and to describe the anisotropy in the FM sublattices the solutions given by the standard theory for an AFM resonance [10] are not sufficient. We are not aware of any published approach which would be applicable to $GdRh_2Si_2$. Therefore, we derived an antiferromagnetic resonance condition for this anisotropy as described in Appendix B. The mean-field model that describes the magnetization of the system [8] together with the resonance condition (B2) predicts the sine-like modulation with excellent quantitative consistency, as demonstrated by the red solid line in the bottom frame of Fig. 4 which depicts the best fit with $\xi = 0$ of Eq. (B9). The situation can also be described by including the dynamics of the system, which is demonstrated in Appendix C. This yields the green solid line with $\xi = -1$ for the precession of the order parameter on an exact circle around its equilibrium direction. For an elliptic precession we expect a different value, such as $\xi = 0$, which fits the data slightly better. Due to a lack of magnetization data, we are not able to determine the restoring force in the basal plane acting on the order parameter which would be necessary to determine the eccentricity of its elliptic orbit.

The mean-field model [8] shows that the values of B_D and B_M (see Appendix B, Fig. 5) are different for different AFM domains. When approaching the [110] direction, the energy difference between the domains decreases, and according to the domain distribution estimated by the Ising chain model [8], the domains coexist. On the other hand, by approaching the [100] direction, the predicted values of B_D and B_M become almost equal, such that the magnetic resonance frequency of both domains becomes similar, too. The structure in the angle dependence of the linewidth around $\vartheta = 45°, 135°$ may therefore be due to a superposition and exchange narrowing of anisotropic resonance signals arising from different domains. A similar behavior was suggested for $CdCr_2S_4$, in which four resonance fields are combined via exchange narrowing into one line [21].

IV. SUMMARY

$GdRh_2Si_2$ is an exemplary tetragonal system for easy-plane magnetic order with a weak in-plane magnetic anisotropy. We investigated the temperature dependence of the resonance field of two in-plane directions as well as the in-plane and out of-plane anisotropies. We found that standard textbook approaches cannot describe the data satisfactorily. Our presented modeling is restricted to the a-a plane and is sufficient to explain one of the two resonance modes. In order to completely describe the magnetization dynamics detailed knowledge about not only the weak in-plane anisotropy [8]

but also the strength of the out-of-plane forces is necessary. We have worked out in detail how the magnetic resonance shifts due to a characteristic property of the system, namely, the retardation of the magnetization when the sample is rotated in an external field. We gave a complete description of this particular effect using closed analytical formulas. This torque effect is not clearly worked out in the literature and can nicely be observed in $GdRh_2Si_2$ because pure single crystals were available and because of the absence of hysteresis in the magnetization. Our investigations of the weak in-plane anisotropy can serve as an interesting illustration of what happens with the dynamics of the order parameter as the anisotropy restrictions become very soft.

ACKNOWLEDGMENTS

K.K. and C.K. gratefully acknowledge support from the DFG(DE) through Grant No. KR3831/5-1. We acknowledge helpful discussions with C. Geibel, H.-A. Krug von Nidda, and Z. Wang. We are particularly grateful to D. Ehlers for his generous help and interest.

APPENDIX A: INTERNAL EXCHANGE FIELD IN THE AFM PHASE

In Ref. [8] a free-energy-based model to describe the AFM phase of $GdRh_2Si_2$ was introduced. The free energy is

$$\begin{aligned} F &= -TS - \tfrac{1}{2}(\mathbf{M}_A + \mathbf{M}_B)\cdot\mathbf{B} + \phi(\mathbf{M}_A,\mathbf{M}_B) \\ &= -TS - \tfrac{1}{2}(\mathbf{M}_A + \mathbf{M}_B)\cdot\mathbf{B} + E_{\mathrm{FM}} + E_{\mathrm{AFM}} + F_{\mathrm{an}}, \end{aligned}$$

with the contribution within a plane

$$E_{\mathrm{FM}} = -\frac{3k_B}{\mu_{\mathrm{eff}}^2}(\Theta_W + T_N)\frac{1}{8}\left(\mathbf{M}_A^2 + \mathbf{M}_B^2\right)$$

and between planes

$$E_{\mathrm{AFM}} = -\frac{3k_B}{\mu_{\mathrm{eff}}^2}(\Theta_W - T_N)\frac{1}{4}(\mathbf{M}_A\cdot\mathbf{M}_B).$$

The anisotropic part F_{an} will be neglected for the discussion of the c direction. We consider the field that is produced by a ferromagnetic plane B and acts on an ion of the sublattice A,

$$\begin{aligned} F &= \underbrace{-\frac{1}{2}\mathbf{M}_A\cdot\mathbf{B}}_{\text{Zeeman Term}} \underbrace{-\frac{3k_B}{\mu_{\mathrm{eff}}^2}(\Theta_W - T_N)\frac{1}{4}(\mathbf{M}_A\cdot\mathbf{M}_B)}_{\text{between layers}} + \cdots \\ &= -\frac{1}{2}\mathbf{M}_A\Bigg[\mathbf{B} + \underbrace{\frac{3k_B}{\mu_{\mathrm{eff}}^2}(\Theta_W - T_N)\frac{1}{2}\mathbf{M}_B}_{\mathbf{B}_{\mathrm{interior,B}}}\Bigg] + \cdots. \end{aligned}$$

In the following, we determine the magnetization $\mathbf{M}_B$ of one ferromagnetic layer. We have

$$M^2 + D^2 = D_0^2, \qquad D_0 = M_{\mathrm{sat}}\sqrt{1 - \frac{T}{T_N}},$$

with $M_{\mathrm{sat}} = 7\,\mu_{\mathrm{B}}$. For the field along the c direction we have $\mathbf{M} \perp \mathbf{D}$, and in particular

$$M(B) = \chi_\perp B_z.$$

This results in

$$\mathbf{M}_A = (D,0,M) = \left(\sqrt{D_0^2 - (\chi_\perp B_z)^2},0,\chi_\perp B_z\right),$$

$$\mathbf{M}_B = (-D,0,M).$$

Therefore, we have

$$\begin{aligned} \mathbf{M} &= \tfrac{1}{2}(\mathbf{M}_A + \mathbf{M}_B) = (0,0,M), \\ \mathbf{D} &= \tfrac{1}{2}(\mathbf{M}_A - \mathbf{M}_B) = (D,0,0). \end{aligned}$$

For the choice of the coordinate system see Fig. 8 in Ref. [8]. The field that acts on an ion of sublattice A, which is created by sublattices A and B, reads

$$\begin{aligned} &\mathbf{B}_{\mathrm{interior,A,B}}(T,B_z) \qquad \text{(A1)} \\ &= -2\frac{\partial}{\partial\mathbf{M}_A}[E_{\mathrm{FM}} + E_{\mathrm{AFM}}] \\ &= \frac{3k_B}{\mu_{\mathrm{eff}}^2}\left[\Theta_W\,\tfrac{1}{2}(\mathbf{M}_A + \mathbf{M}_B) + T_N\,\tfrac{1}{2}(\mathbf{M}_A - \mathbf{M}_B)\right] \\ &= \frac{3k_B}{\mu_{\mathrm{eff}}^2}\left\{\frac{\Theta_W}{2}\mathbf{M} + \frac{T_N}{2}\mathbf{D}\right\} \\ &= \frac{3k_B}{\mu_{\mathrm{eff}}^2}\begin{pmatrix} T_N\sqrt{M_{\mathrm{sat}}^2(1 - T/T_N) - (\chi_\perp B_z)^2} \\ 0 \\ \Theta_W\,\chi_\perp B_z \end{pmatrix}. \qquad \text{(A2)} \end{aligned}$$

The values of $\Theta_W = 8\,\mathrm{K}$, $T_N = 107\,\mathrm{K}$, $\mu_{\mathrm{eff}} = 8.28\mu_{\mathrm{B}}$, and $\chi_\perp = 0.149\mu_{\mathrm{B}}/\mathrm{T}$ have been determined by magnetic measurements [6,8].

APPENDIX B: IN-PLANE ANISOTROPY

This appendix derives a fit formula using a general ansatz without knowledge of the dynamics. In the following, we consider the behavior of one domain. We use the mean-field model developed in Ref. [8] to predict the ESR resonance field for an external field $\mathbf{B}$ applied perpendicular to the crystallographic [001] direction. The free energy

$$\begin{aligned} F(\varphi) \;=\; & F_0(D_0) - \frac{B^2}{4}(\chi_\perp + \chi_\parallel) - \frac{B^2}{4}(\chi_\perp - \chi_\parallel)u \\ & + \frac{B_{\mathrm{sf}}^2}{8}(\chi_\perp - \chi_\parallel)\sin^2 2\varphi, \end{aligned}$$

with $u = -\cos(2\vartheta - 2\varphi)$, where B_{sf}, $\chi_\perp$, and $\chi_\parallel$ are temperature dependent, Eq. (6) [8], and the magnetization

$$\mathbf{M} = \hat{\chi}\mathbf{B} = \chi_\perp(1 - \mathbf{e}_D\otimes\mathbf{e}_D)\mathbf{B} + \chi_\perp\,\mathbf{e}_D\otimes\mathbf{e}_D\,\mathbf{B},$$

Eq. (4) [8], serve as the starting point. See Fig. 5 for the choice of the coordinate system. For our purpose it is sufficient to ignore $\chi_\parallel$. The ESR interaction is so fast that we do not expect an isothermic relaxation. Here, only $\chi_\perp$ is relevant since this keeps the entropy unchanged. Therefore, the magnetization becomes

$$\mathbf{M} = \chi_\perp B_M \mathbf{e}_M,$$

with $B_M = \mathbf{B} \cdot \mathbf{e}_M$ for $\mathbf{B}$ aligned perpendicular to the [001] direction. The free energy

$$F(\varphi) = F_0 - \chi_\perp \frac{B^2}{4} [\, 1 - \cos(2\vartheta - 2\varphi) \,] + \chi_\perp \frac{B_{\rm sf}^2}{8} \sin^2 2\varphi$$

can be minimized with respect to φ

$$\frac{\partial}{\partial \varphi} F(\varphi) = \chi_\perp \frac{B^2}{2} \sin(2\vartheta - 2\varphi) + \chi_\perp \frac{B_{\rm sf}^2}{4} \cos 2\varphi \, \sin 2\varphi = 0.$$

With $B_D = B \cos(\vartheta - \varphi)$ and $B_M = -B \sin(\vartheta - \varphi)$ the minimum condition reads

$$-B_D \, B_M + \tfrac{1}{4} B_{\rm sf}^2 \sin 4\varphi = 0. \tag{B1}$$

The decomposition of $B = B_{\rm ext}$ (Fig. 5) into B_D and B_M is done with respect to one AFM domain which consists of two FM sublattices. In the paramagnetic regime, the ESR frequency ω can be decomposed in the following way: The square of ω is the sum of three parts that arise from the three components of the external field. This reads

$$\omega^2 = \omega_x^2 + \omega_y^2 + \omega_z^2,$$

with

$$\omega_x = \gamma \, B_x, \quad \omega_y = \gamma \, B_y, \quad \omega_z = \gamma \, B_z.$$

We deduce a similar ansatz to describe the ESR frequency in the ordered regime. In particular, we describe the ESR behavior of one certain domain. First of all, we introduce $\omega_{\rm field}$ and take into account that the external magnetic field decomposes into a parallel component B_D and orthogonal component B_M with respect to the ordering parameter $\mathbf{D}$. Furthermore, we account for the anisotropy in the system by utilizing $\omega_{\rm aniso} = \omega_{\rm aniso}(\varphi)$, which is a function of the order parameter φ. These considerations lead to the ansatz

$$\omega^2 = \omega_{\rm aniso}^2 + \omega_{\rm field}^2(\mathbf{B}).$$

An arbitrary analytic function that respects the symmetry of one domain has the form

$$\phi(\mathbf{B}) = \phi_0 + c_D \, B_D^2 + c_M \, B_M^2,$$

and we can write

$$\omega_{\rm field}^2(\mathbf{B}) = \gamma_D^2 \, B_D^2 + \gamma_M^2 \, B_M^2.$$

For symmetry reasons, there is a $\pi/2$ periodicity upon rotations in the basal plane of the tetragonal lattice, such that

$$\omega_{\rm aniso}^2 = \omega_{0,\rm an}^2 + \omega_{1,\rm an}^2 \cos 4\varphi,$$

where we take the constant and the first nonvanishing term of the Fourier series into account. Summation yields

$$\omega^2 = \omega_{0,\rm an}^2 + \omega_{1,\rm an}^2 \cos 4\varphi + \gamma_D^2 \, B_D^2 + \gamma_M^2 \, B_M^2 \tag{B2}$$

for the resonance frequency. To introduce the amplitudes into the fit formula, we use the [100] direction, where the resonance field has its maximum $B_{\rm max}$, and the [110] direction, where the resonance field has its minimum $B_{\rm min}$. We choose the coordinate system such that φ is the angle between the [110] direction and the ordering vector $\mathbf{D}$. In both cases, the external field is parallel to a main symmetry axis, such that $B = B_M$. This leads to

$$\omega^2 = \omega_{0,\rm an}^2 - \omega_{1,\rm an}^2 + \gamma_D^2 \, B_D^2 + \gamma_M^2 \, B_{\rm max}^2,$$
$$\omega^2 = \omega_{0,\rm an}^2 + \omega_{1,\rm an}^2 + \gamma_D^2 \, B_D^2 + \gamma_M^2 \, B_{\rm min}^2.$$

From these two equations we determine

$$\omega^2 - \omega_{0,\rm an}^2 = \gamma_M^2 \, \tfrac{1}{2} \big(B_{\rm max}^2 + B_{\rm min}^2 \big),$$
$$\omega_{1,\rm an}^2 = \gamma_M^2 \, \tfrac{1}{2} \big(B_{\rm max}^2 - B_{\rm min}^2 \big).$$

With Eq. (B2) we get

$$\tfrac{1}{2} \big(B_{\rm max}^2 + B_{\rm min}^2 \big) - \tfrac{1}{2} \big(B_{\rm max}^2 - B_{\rm min}^2 \big) \cos 4\varphi = \xi \, B_D^2 + B_M^2, \tag{B3}$$

with the parameter $\xi = (\gamma_D / \gamma_M)^2$ to be determined by fitting. To parametrize the plot in φ, which is the angle between the x axis ([110] direction) and the direction of the ordering vector $\mathbf{D}$, we rewrite Eqs. (B1) and (B3) and get

$$B_M^2 + \xi \, B_D^2 = A_1, \tag{B4}$$

$$B_M \, B_D = A_2, \tag{B5}$$

with

$$A_1 := \tfrac{1}{2} \big(B_{\rm max}^2 + B_{\rm min}^2 \big) - \tfrac{1}{2} \big(B_{\rm max}^2 - B_{\rm min}^2 \big) \cos 4\varphi \tag{B6}$$

and

$$A_2 := \tfrac{1}{4} B_{\rm sf}^2 \sin 4\varphi. \tag{B7}$$

To solve these equations we multiply Eq. (B4) by B_M^2 and get a quadratic equation,

$$B_M^4 + \xi \, A_2^2 = A_1 \, B_M^2.$$

From the two solutions we use the larger one,

$$B_M^2 = \frac{A_1}{2} + \sqrt{\frac{A_1^2}{4} - \xi \, A_2^2},$$

such that $|B_D| < |B_M|$ is fulfilled. Now we compute the component of the external field that is parallel to $\mathbf{D}$:

$$B_D^2 = \frac{A_2^2}{B_M^2} = \frac{1}{\xi} \left\{ \frac{A_1}{2} - \sqrt{\frac{A_1^2}{4} - \xi \, A_2^2} \right\}.$$

This yields the square of the external field for the resonance condition:

$$B_{\rm res}^2 = B_M^2 + B_D^2 = \left(\frac{1}{2} + \frac{1}{2\xi} \right) A_1 + \left(\frac{1}{2} - \frac{1}{2\xi} \right) \sqrt{A_1^2 - 4 \, \xi \, A_2^2}. \tag{B8}$$

Since we have

$$B_M = B_{\rm res} \cos(\vartheta - \varphi), \quad B_D = B_{\rm res} \sin(\vartheta - \varphi),$$

we get

$$A_2 = B_M \, B_D = \tfrac{1}{2} B_{\rm res}^2 \sin(2\vartheta - 2\varphi).$$

With this we get a relation between the resonance field $B_{\rm res}$ and the angle ϑ between the external field and the [110]

direction,

$$\vartheta = \varphi + \frac{1}{2}\arcsin\frac{2A_2}{B_{\rm res}^2}, \tag{B9}$$

using Ens. (B6), (B7), and (B8). For $\xi \to 0$ (and $\gamma_D \to 0$) the ESR data are described well by Eq. (B9), as shown by the red line in the bottom frame of Fig. 4. The precession of the order parameter on a circle around its equilibrium direction leads to $\xi = -1$.

APPENDIX C: DYNAMICS OF THE ORDER PARAMETER

A particular model which describes the motion of the order parameter in the a-a plane is presented in this appendix. This model fixes the four parameters $\omega_0, \omega_{\rm an}, \gamma_D$, and γ_M (Appendix B), and only one parameter, γ, remains.

The free energy [8] is

$$F = F_0 - \chi_\perp \frac{B^2}{4}\left[1 - \cos(2\vartheta - 2\varphi)\right] + \chi_\perp \frac{B_{\rm sf}^2}{8}\sin^2 2\varphi,$$

where φ is the direction of the antiferromagnetic order parameter. With

$$B_D = B\,\cos(\vartheta - \varphi),$$
$$B_M = -B\,\sin(\vartheta - \varphi),$$

we rewrite F according to

$$F(\varphi) = F_0 - \frac{\chi_\perp}{2} B_M^2 + \chi_\perp \frac{B_{sf}^2}{8}\sin^2 2\varphi. \tag{C1}$$

We expand F around its minimum at φ_0 up to second order in φ. Using

$$\frac{\partial B_D}{\partial \varphi} = -B_M, \quad \frac{\partial B_M}{\partial \varphi} = B_D,$$

we obtain the first and second derivatives of F with respect to the direction of the order parameter,

$$\frac{\partial F}{\partial \varphi} = -\chi_\perp B_D B_M + \chi_\perp \frac{1}{2}\sin 2\varphi \cos 2\varphi,$$
$$\frac{\partial^2 F}{\partial \varphi^2} = \chi_\perp (B_M^2 - B_D^2) + \chi_\perp B_{\rm sf}^2 \cos 4\varphi.$$

The direction of the order parameter is described by two canonical spatial variables and two conjugated momentum variables. For an oscillating system this results in two eigenfrequencies. The model [8] is restricted to the a-a plane, and only one of the dynamical variables is accessible for us. Therefore, we can expect to explain one of the two resonance modes. We have the dynamical variable

$$\mathbf{e}_D = (\cos\varphi\,,\ \sin\varphi),$$

and the projection of the external field $\mathbf{B} = B(\cos\vartheta\,,\ \sin\vartheta)$ into the order parameter direction

$$B_D = \mathbf{e}_D \cdot \mathbf{B}.$$

The Larmor energy is

$$E_{\rm LM} = \frac{\chi_\perp}{2}(\mathbf{e}_D \cdot \mathbf{B})^2 + \frac{\chi_\perp}{2}\frac{\dot{\mathbf{e}}_D^2}{\gamma^2},$$

where the first part is a potential due to the external field and the second part is the kinetic energy due to the change in the order parameter. The anisotropy contribution is

$$E_{\rm an} = \chi_\perp \frac{B_{\rm sf}^2}{8}\sin^2 2\varphi = U.$$

For small displacements for the direction of the order parameter $\Delta\varphi(t)$ with the ansatz

$$\varphi = \varphi_0 + \Delta\varphi(t)$$

we have

$$\dot{\mathrm{e}}_D^2 = (\Delta\dot{\varphi})^2.$$

The approximation around the minimum is

$$\begin{aligned} E &= E_{\rm LM} + E_{\rm an} \\ &= \frac{1}{2}\frac{\partial^2 F}{\partial \varphi}(\varphi - \varphi_0)^2 + \frac{\chi_\perp}{2}\frac{\dot{\mathbf{e}}_D^2}{\gamma^2} \\ &= \frac{1}{2}\frac{\partial^2 F}{\partial \varphi^2}(\Delta\varphi)^2 + \frac{1}{2}\frac{\chi_\perp}{\gamma^2}\Delta\dot{\varphi}^2, \end{aligned}$$

which is the energy of a harmonic oscillator. The frequency of this harmonic oscillator is the ESR resonance frequency $\omega_{\rm res}$, determined by

$$\frac{\partial^2 F}{\partial \varphi^2} = \frac{\chi_\perp}{\gamma^2}\omega_{\rm res}^2.$$

Being more explicit, we get

$$\gamma^2\left(B_M^2 - B_D^2\right) + \gamma^2 B_{\rm sf}^2 \cos 4\varphi = \omega_{\rm res}^2. \tag{C2}$$

Our ansatz in (B2),

$$\omega_{\rm res}^2 = \omega_{0,\rm an}^2 + \omega_{1,\rm an}^2 \cos 4\varphi + \gamma_D^2 B_D^2 + \gamma_M^2 B_M^2, \tag{C3}$$

has four parameters, $\omega_{0,\rm an}$, $\omega_{1,\rm an}$, γ_D, and γ_M. Equation (C2) contains only one parameter, which fixes three of our parameters. A comparison with Eq. (C3) yields

$$\omega_{0,\rm an}^2 = 0,\ \omega_{1,\rm an}^2 = \gamma^2 B_{\rm sf}^2,\ \gamma_D^2 = -\gamma^2,\ \gamma_M^2 = \gamma^2,$$

$$\xi = -1.$$

The green line in the bottom frame of Fig. 4 illustrates how this result fits the data.

[1] O. Trovarelli, C. Geibel, S. Mederle, C. Langhammer, F. M. Grosche, P. Gegenwart, M. Lang, G. Sparn, and F. Steglich, Phys. Rev. Lett. **85**, 626 (2000).

[2] S. Quezel, J. Rossat-Mignod, B. Chevalier, P. Lejay, and J. Etourneau, Solid State Commun. **49**, 685 (1984).

[3] T. Shigeoka, T. Fujiwara, K. Munakata, K. Matsubayashi, and Y. Uwatoko, J. Phys. Conf. Ser. **273**, 012127 (2011).

[4] A. Generalov, M. M. Otrokov, A. Chikina, K. Kliemt, K. Kummer, M. Höppner, M. Güttler, S. Seiro, A. Fedorov, S. Schulz, S. Danzenbächer, E. V. Chulkov, C. Geibel, C. Laubschat, P. Dudin, M. Hoesch, T. Kim, M. Radovic, M. Shi, N. C. Plumb, C. Krellner, and D. V. Vyalikh, Nano Lett. **17**, 811 (2017).

[5] A. Chikina, A. Generalov, K. Kummer, M. Güttler, V. N. Antonov, Y. Kucherenko, K. Kliemt, C. Krellner, S. Danzenbächer, T. Kim, P. Dudin, C. Geibel, C. Laubschat, and D. V. Vyalikh, Phys. Rev. B **95**, 155127 (2017).

[6] K. Kliemt and C. Krellner, J. Cryst. Growth **419**, 37 (2015).

[7] G. Czjzek, V. Oestreich, H. Schmidt, K. Łatka, and K. Tomala, J. Magn. Magn. Mater. **79**, 42 (1989).

[8] K. Kliemt, M. Hofmann-Kliemt, K. Kummer, F. Yakhou-Harris, C. Krellner, and C. Geibel, Phys. Rev. B **95**, 134403 (2017).

[9] M. Güttler, A. Generalov, M. M. Otrokov, K. Kummer, K. Kliemt, A. Fedorov, A. Chikina, S. Danzenbächer, S. Schulz, E. V. Chulkov, Y. M. Koroteev, N. Caroca-Canales, M. Shi, M. Radovic, C. Geibel, C. Laubschat, P. Dudin, T. K. Kim, M. Hoesch, C. Krellner, and D. V. Vyalikh, Sci. Rep. **6**, 24254 (2016).

[10] A. Gurevich and G. Melkov, *Magnetization Oscillations and Waves* (CRC Press, Boca Raton, New York, 1996).

[11] E. Turov, *Physical Properties of Magnetically Ordered Crystals*, edited by A. Tybulewicz and S. Chomet (Academic, New York, 1965).

[12] V. Glazkov, T. Soldatov, and Y. Krasnikova, Appl. Magn. Reson. **47**, 1069 (2016).

[13] A. I. Pankrats, D. Y. Sobyanin, A. M. Vorotinov, and G. A. Petrakovskii, Solid State Commun. **109**, 263 (1998).

[14] D. Rauch, M. Kraken, F. J. Litterst, S. Süllow, H. Luetkens, M. Brando, T. Förster, J. Sichelschmidt, A. Neubauer, C. Pfleiderer, W. J. Duncan, and F. M. Grosche, Phys. Rev. B **91**, 174404 (2015).

[15] J. Sichelschmidt, K. Kliemt, C. Krellner, and C. Geibel, J. Phys.: Conf. Ser. **807**, 012007 (2017).

[16] B. Elschner and A. Loidl, *Electron-Spin Resonance on Localized Magnetic Moments in Metals* (Elsevier, Amsterdam, 1997), Chap. 162, p. 221.

[17] D. L. Huber, Mod. Phys. Lett. B **26**, 1230021 (2012).

[18] E. Kwapulińska, K. Kaczmarska, and A. Szytuła, J. Magn. Magn. Mater. **73**, 65 (1988).

[19] H. Benner and J. P. Boucher, in *Magnetic Properties of Layered Transition Metal Compounds*, edited by L. J. De Jongh, Physics and Chemistry of Materials with Low-Dimensional Structures Vol. 9 of Magnetic Properties of Layered Transition Metal Compounds (Kluwer, Dordrecht, 1990), pp. 323–378.

[20] A. Abragam and B. Bleaney, *Electron Paramagnetic Resonance of Transition Ions* (Clarendon, Oxford, 1970).

[21] D. Ehlers, V. Tsurkan, H.-A. Krug von Nidda, and A. Loidl, Phys. Rev. B **86**, 174423 (2012).